



Microtomography study of magnesium friction stir welding procedure and magnesium alloys

Katarzyna Fornal¹, Pavel Lytaev²

¹Jagiellonian University, Poland

²Moscow Institute of Physics and Technology, Russia

Supervisor:

Felix Beckmann

September 7, 2011

Abstract

Microtomography due to its ability of non-invasive study of the internal structure of the sample is a technique widely applied for example in the materials science area. In this report the results of investigation of magnesium samples are presented. Using a computed microtomography system, friction stir welding samples and magnesium alloys samples were examined. The obtained tomography reconstructions visualize the distribution of titanium particles used as a marker in the friction stir welding process and cracks in magnesium alloys, which appeared during casting procedure.

Contents

1	Introduction	3
1.1	Motivation	3
1.2	Friction stir welding	3
1.3	Magnesium alloys processing	4
2	Methods	4
2.1	Tomography	4
2.2	Microtomography using X-ray tubes and synchrotron radiation	6
3	Samples	7
3.1	Friction stir welding samples	7
3.2	Magnesium alloy samples	7
4	Experimental part	8
4.1	Experimental setup	8
4.2	Tomographic scans	9
4.3	Reconstruction	9
4.4	Processing of data	10
5	Results and Discussions	10
5.1	Friction stir welding samples	10
5.2	Magnesium alloys samples	12
6	Conclusions	15
7	Acknowledgements	15
	References	15

1 Introduction

1.1 Motivation

Magnesium is the lightest useful metal, so it is excellent to use in several applications especially in the automotive and aerospace, where fuel economy and weight reduction are very important. However, the possibility of corrosion, the fragility and the fact that magnesium is very hard to deform at ambient temperature limit the development of the magnesium alloys application.

For this reason in recent years, interest has increased in development of the new joining methods of magnesium e.g. friction stir welding but also in alloy development and optimisation of processing technologies.

In those researches very useful is microtomography technique, which allows to investigate the results of friction stir welding and examine the material quality, like the morphology of cracks or distribution of different alloy component.

1.2 Friction stir welding

Friction stir welding (FSW) is a sophisticated and innovative welding technology invented and experimentally proven by Wayne Thomas and a team of his colleagues at The Welding Institute (UK) in 1991. Friction-stir welding is a solid-state joining method in which the metal is not melted during the process but only is plasticized. It is especially useful on large pieces of light metals e.g. aluminium and magnesium.

In the friction stir welding process, a tool, with a probe attached to its tip, is rotated at a constant speed and moved at a constant speed along the joint line between two pieces of material plate, which are welded (Fig. 1).

The frictional heat generated by this process softens the metal to produce a plastic flow that effectively stirs the metal from both pieces of plate and melding them together to create a weld. Due to the fact that friction stir welding is a solid-state welding method it results in a low concentration of defects, a low deformation and excellent mechanical properties of welded material.

The most important advantages of the friction stir welding method are good mechanical properties of welded material, energy savings, improving of the working environment and the low environmental impact.

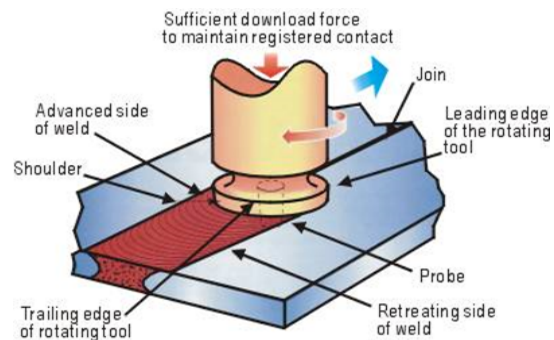


Figure 1: Schematic diagram of the friction stir welding process [1].

1.3 Magnesium alloys processing

One of the kinds of metal processing is casting process by which a liquid material is poured into a mold and then allowed to solidify. Casting is most often used for metals and alloys. This process allows making complex shapes that would be otherwise difficult or uneconomical to make by other methods. However, the heat treatment of the material may cause residual stresses that may result in distortion or cracking. Therefore it is very important to optimize casting conditions such as a temperature of the melted alloy and a quenching temperature and also alloy details.

2 Methods

2.1 Tomography

Soon after the discovery of X-ray the method of X-ray tomography was developed. This is one of the most visible and beautiful techniques that use X-rays. In fact, this is a non-invasive method for studying the internal structure of the sample with the possibility of constructing the slices of the object in any plane or getting its three-dimensional reconstruction. The principle of this method is to obtain a sequence of X-ray projections of the object as it rotates around an axis perpendicular to the beam of the X-ray radiation. The scheme of such tomographic experiment is shown in Figure 2 .

Then with a help of the specialized software, based on the mathematical principles of tomography, the slices of the object and its three-dimensional image can be reconstructed from these projections. Nowadays this technique is widely applied in many fields of science and medicine. There is a huge variety of specialized technical equipment, devices and management software. That all is necessary for the study of objects of different nature and sizes from particulate organic matter to large metal samples from the grains of crystals to a live person. Of course, in each case this requires its own setup and the specificity of the experiment. Depending on the properties of the object the parameters such as X-ray beam energy (the choice of a suitable source), the maximum time of irradiation with consideration of the permissible dose (rotation speed of the object) and the spatial resolution (peculiarities of the detector) may vary. The general principle of the tomographic experiment, however, remains the same in all cases, moreover, it even extends to the case of non-X-ray sources, such as magnetic resonance imaging.

In the year 1917 J. Radon has published the following mathematical transformations, called Radon-Transformation:

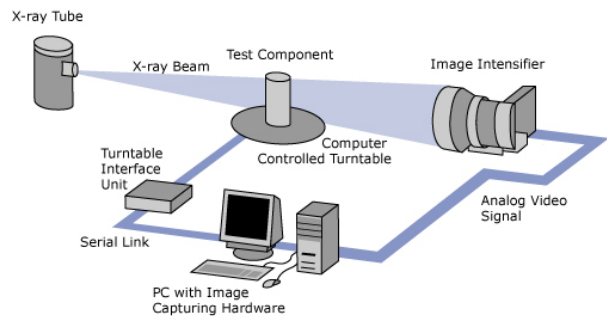


Figure 2: General scheme of the tomographic experiment.

$$p_{\theta}(t) = \int_{-\infty}^{\infty} \int_{-\infty}^{\infty} dx dy df(x, y) \delta(x \cos \theta + y \sin \theta - t) = \int_{-\infty}^{\infty} ds f(x = t \cos \theta, y = t \sin \theta) \quad (1)$$

They allow to interpret mathematically the intensity distribution of the parallel projections of an object, that is, the pictures obtained by passing a parallel X-ray beam through the object (Fig. 3).

In addition, we know that X-ray radiation is absorbed by the substance as follows:

$$I = I_0 \cdot e^{-\Delta x \mu_1} \cdot e^{-\Delta x \mu_2} \cdot e^{-\Delta x \mu_3} \dots = I_0 \cdot e^{-\sum_i \Delta x \mu_i} \quad (2)$$

In the case of a continuous distribution of various substances in the sample, replace the sum by an integral:

$$I = I_0 \cdot e^{-\int ds \mu(x, y)} \quad (3)$$

Thus, the unknown function, were part of the Radon-Transformation, is as follows:

$$p_{\theta}(t) = \ln\left(\frac{I}{I_0}\right) = - \int ds \mu(x, y) \quad (4)$$

The intermediate result of the reconstruction of two-dimensional pattern is called a sinogram of the object. This is a way to sort the data in a form suitable for image reconstruction. In fact, this two-dimensional image slice of all the one-dimensional projections of the object is a function of projection angle (the angle at which the projection is measured). The projection angle is depicted on the ordinate, linear coordinate projection is depicted on the abscissa. The principle of obtaining the sinogram is illustrated in Figure 4.

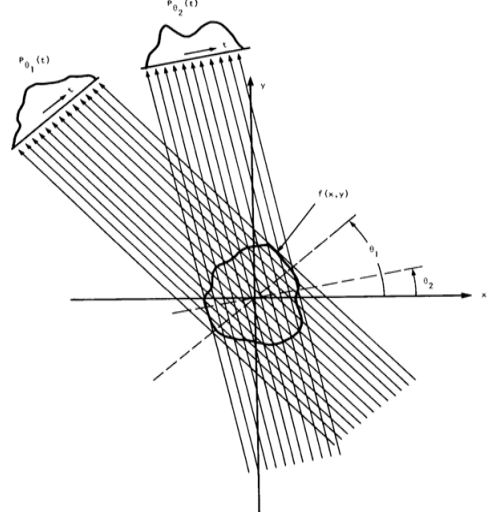


Figure 3: Parallel-projection for the derivation of Random-Transformation.

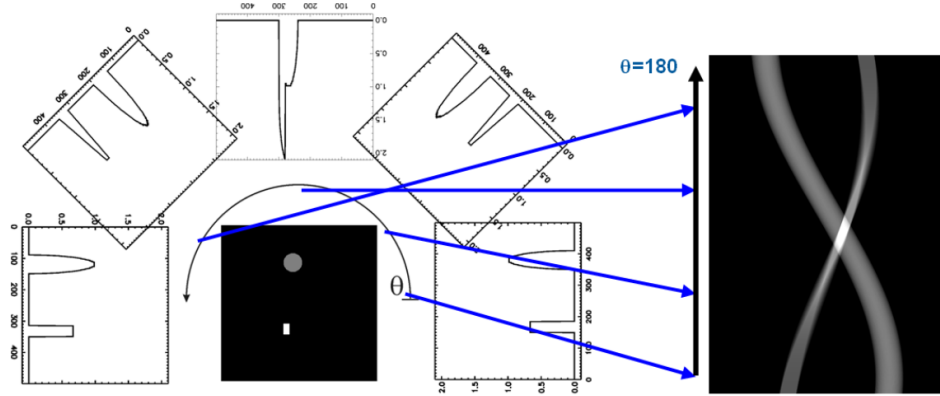
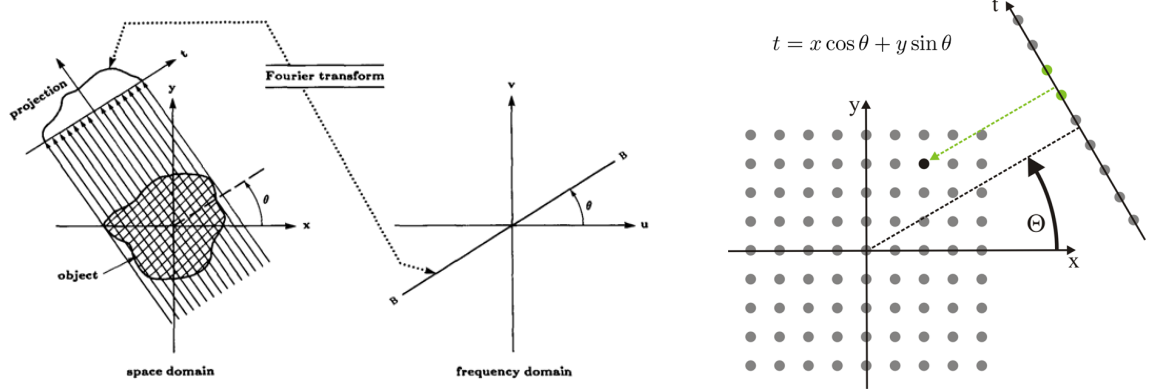


Figure 4: Tomographic projections and obtained sinogram.

Then, in fact, left only to reconstruct the original pattern of distribution of matter in the sample from the known function $P_\theta(t)$. For this purpose uses the conversion, based on the consistent application of 1D-Fourier-transformation and Fourier-Scheiben-Theorem (Fig. 5(a) and eq. 5).

$$F(u, v) = \int_{-\infty}^{\infty} \int_{-\infty}^{\infty} dx dy f(x, y) e^{-2\pi i(ux+vy)} \quad (5)$$



(a) 1D-Fourier-transformation of the single projection, $p_\theta(t) \Rightarrow f(x, y)$ (layer), $P_\theta(w) = F(w, \theta)$, $F(w, \theta)$ is polarpicture of Fourier-transformed function $F(u, v)$.

(b) The $P_\theta(w)$ Fourier-transform of the projection of $p_\theta(t)$, linear interpolation.

Figure 5

Then, after some calculations that we omit and performing the change of variables $u = w \cos \theta$, $v = w \sin \theta$, $du dv = w dw d\theta$, one can obtain the formula, which can give us the $f(x, y)$ from the projections obtained in the experiment (eq. 6). For a linear discrete case it is illustrated in Figure 5(b).

$$f(x, y) = \int_0^\theta d\theta \int_{-\infty}^{\infty} dw |w| P_\theta(w) e^{i2\pi w t} \quad (6)$$

2.2 Microtomography using X-ray tubes and synchrotron radiation

As already stated, for each kind of samples, which have to be investigated by the method of X-ray tomography, it is necessary to provide the special and sometimes unique conditions of the experiment. In case we can achieve high spatial resolution of about one micrometer in our experiment (of X-ray tomography), such method usually is called microtomography. As X-ray sources, either X-ray tube or a channel of a synchrotron source is used. X-ray tubes are certainly much cheaper and more accessible to use, but the synchrotron radiation has several advantages, which are sometimes simply necessary to achieve the desired result. In such cases, even the best and most expensive X-ray tubes are not suitable for the experiment. These advantages are primarily in the fact that the synchrotron radiation at the output of the monochromator is monochromatic,

nearly parallel beam of high intensity, which allows us to achieve much higher spatial resolution than using X-ray tube.

In some cases there is no need to use synchrotron radiation sources and device for X-ray microtomography with X-ray tube as a source can be used. This kind of device can provide the required photon energy and also a quite high spatial resolution (of order a few micrometers). It is possible due to the extremely powerful X-ray tube with the special system of focusing of the electron beam. The schema of the X-ray tube use in laboratory microtomography systems is shown in Figure 6.

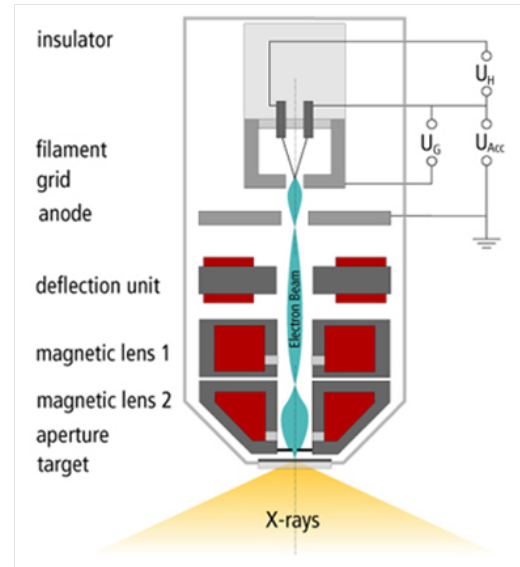


Figure 6: The scheme of the nanofocusing X-ray tube.

3 Samples

3.1 Friction stir welding samples

The friction stir welding samples were prepared by Leon Leander Hutsch from WMP (Institute of Materials Research, HZG Geesthacht, Germany) research group. The investigated samples were magnesium plates including the weld and the weld zone. Samples were produced with different welding speed: 1m/min and 10m/min. Titanium particles with diameter about $40\mu\text{m}$ were used as a marker to investigate movement of magnesium during welding process. Before starting the welding process titanium particles had been inserted on the top of one of the magnesium plates.

3.2 Magnesium alloy samples

The magnesium alloy samples were prepared by dr. A. Srinivasan from Magnesium Innovation Center MagIC (Institute of Materials Research, HZG Geesthacht, Germany) research group, which is conducting research in the magnesium alloy process technology. The investigated samples were pieces of magnesium alloys obtained in casting process selected from the border of areas with different temperature conditions, where cracks appear. There was a hole in the middle of each sample, in which the thermocouple had been placed during the casting. The sample details like alloy composition and temperatures describing the casting conditions are given in Table 1.

Table 1: The description of investigated samples

Sample	Alloy details	Casting conditions
a	Mg-10hd	$T = 250^{\circ}C, T2$
b	Mg-2hd	$T = 250^{\circ}C, T2$
c	Mg-2hd	$T = 250^{\circ}C, T1$
1	Mg-10Gd	$T = 450^{\circ}C, T1$
2	Mg-2Gd	$T = 450^{\circ}C, T2$
3	Mg-1Gd	$T = 450^{\circ}C, T1$
4	Mg-1Gd	$T = 450^{\circ}C, T2$
5	Mg-5Gd	$T = 450^{\circ}C, T2$
6	Mg-0.2Y	$T = 250^{\circ}C, T1$
7	Mg-10.9Y	$T = 250^{\circ}C, T1$
8	Mg-1.5Y	$T = 250^{\circ}C, T1$
9	Mg-2Y	$T = 250^{\circ}C, T2$
10	Mg-4Y	$T = 250^{\circ}C, T1$

4 Experimental part

4.1 Experimental setup

Microtomography measurements were performed using the *nanotom*[®] s (phoenix, GE Measurement & Control Solutions, Germany) nanofocus computed tomography system with *datos|x 2.0 acquisition* (phoenix, GE Measurement & Control Solutions, Germany) interface software (Fig. 7). The *nanotom*[®] s has got the performance nanofocus X-ray tube with max. tube voltage 180V and max. output 15W, which can be operated for the submicron spatial resolution a for high-energy applications for materials science. This device is also equipped with a detector (307x 2 2400 pixel DXR 500L detector), which allows to investigate relatively large objects (up to 250 x 240 mm) with a good spatial resolution.

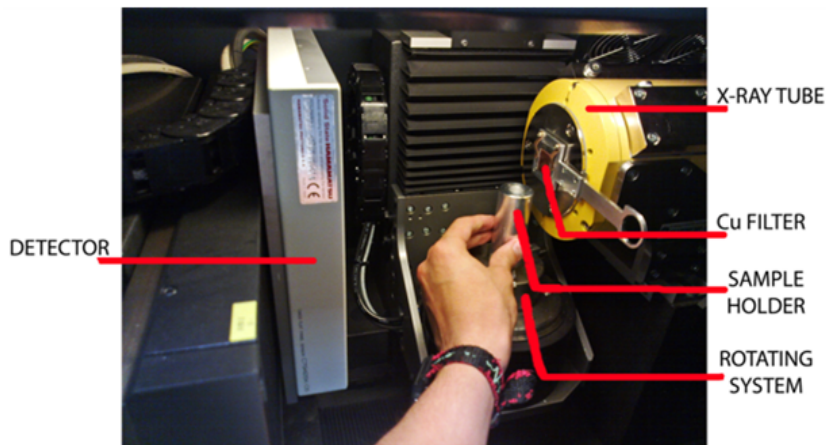


Figure 7: View inside the *nanotom*[®] s computed tomography system.

4.2 Tomographic scans

For each of the tomographic scans a set of 1200 projections at different sample rotations equally stepped between 0° and 360° were measured. The scan parameters like voltage, current and exposure time were selected depending on the sample to use the full detector statistics. The scan parameters for friction stir welding samples have been summarized in Table 2 and for magnesium alloy samples in Table 3.

Table 2: The tomographic scans parameters for friction stir welding samples

Sample	Voltage [V]	Current [mA]	Exposure time [s]
1 - the welding speed 1m/s	160	22	1500
2 - the welding speed 10m/s	160	23	1250

Table 3: The tomographic scans parameters for magnesium alloy samples

Sample	Voltage [V]	Current [mA]	Exposure time [s]
a	160	22	1500
b	160	23	1250
c	160	22	1250
1	165	14	1750
2	161	12	1750
3	140	25	1500
4	160	16	1500
5	155	18	1500
6	142	24	1500
7	140	26	1500
8	150	22	1500
9	148	24	1500
10	148	21	1500

4.3 Reconstruction

The 3D volume reconstruction was calculated from the 2D projections (with a filtered back-projection algorithm) using *datos|x 2.0 reconstruction* (phoenix, GE Measurement & Control Solutions, Germany) software. To improve reconstruction quality the automatic geometry calibration was applied during the reconstruction process. From each set of projections two volume renderings with different reconstruction resolution (1 and 1/2) were created. The reconstruction resolution equal to 1/2 was applied to reduce size of the final file.

4.4 Processing of data

Friction stir welding samples

The visualization of friction stir welding samples was created using special 3D visualization software *VGStudio Max 2.2* (Volume Graphics GmbH, Heidelberg, Germany). To reduce the influence of noise the Gaussian filter was applied to the reconstructed data. 2D slides of samples and the volume rendering of segmented titanium particles were produced. Some animation showing obtained 3D reconstruction of samples and segmented titanium particles was also prepared.

Magnesium alloys samples

For evaluation data of magnesium alloy samples we used *IDL 8.1* (Research Systems Inc., Boulder, CO, USA) software. To compare properties of different samples obtained 3D reconstructions were rescaled to the same gray scale. Several different slides from volume renderings were produced for each sample to visualize cracks occurring in investigated magnesium elements. The image useful to discuss the results containing slides, the gray scale, information about sample and scan parameters was prepared for each sample.

5 Results and Discussions

5.1 Friction stir welding samples

3D reconstructions and segmented titanium particles for both investigated samples are shown in Figure 8. The results obtained with both samples show difference in the distribution and number of titanium particles depending on welding speed. In sample, which was produced with higher speed, titanium particles are distributed mainly on one side of sample. On the other hand in the case of lower welding speed more titanium particles are observed and they are distributed on both side of sample.

The difference in the distribution of titanium particles in samples is visible also on 2D slides (Fig. 9). Highly absorbing titanium particles (white color in grey scale) occur on one or both sides of slides depending on welding speed.

The difference in the distribution of titanium particles may indicate different material flow mechanism for various speeds of welding.

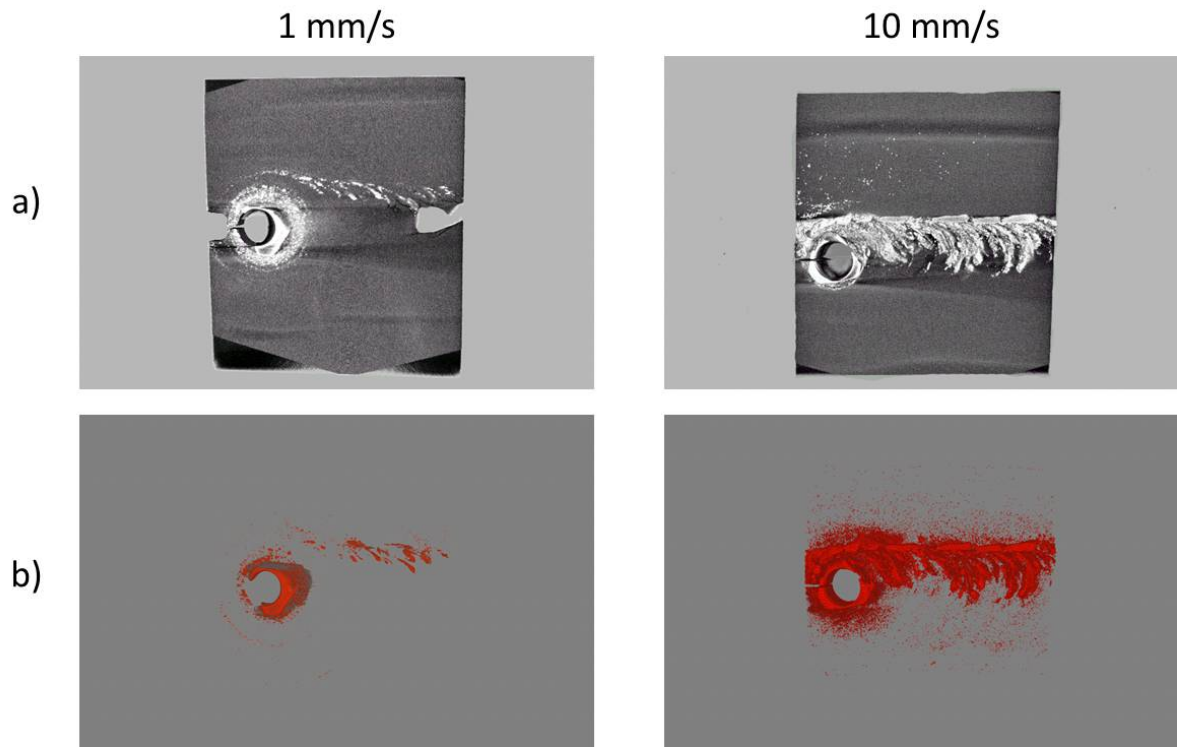


Figure 8: The volume rendering of the friction stir welding samples (a) and the visualisation of the titanium particles (b).

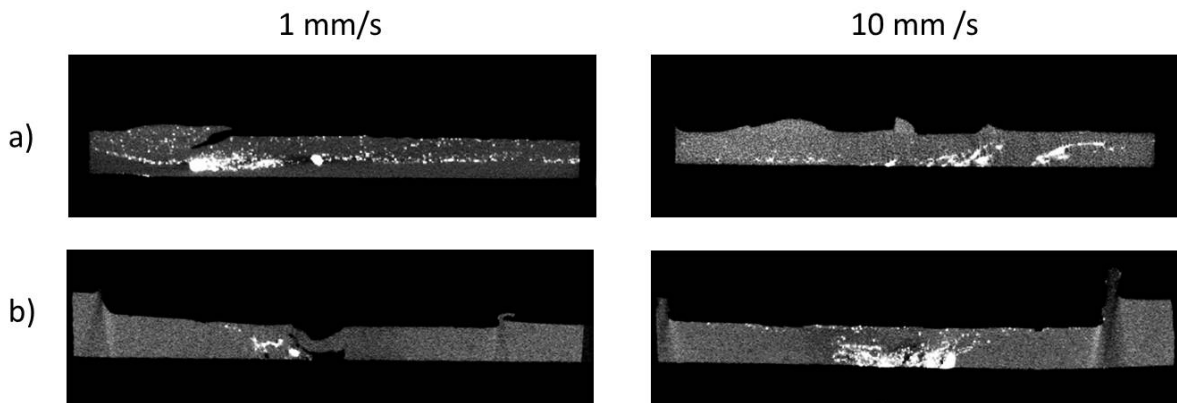


Figure 9: The 2D slides of both samples in two different perpendicular planes (a) and (b).

5.2 Magnesium alloys samples

In Figure 10 a sample image created in IDL 8.1 containing subsequent slides through the magnesium alloy element is shown. The slide position equal to 0.00 represent the position of boundary between two areas with different conditions. The obtained image shows a number, volume and a distribution of cracks in the sample volume.

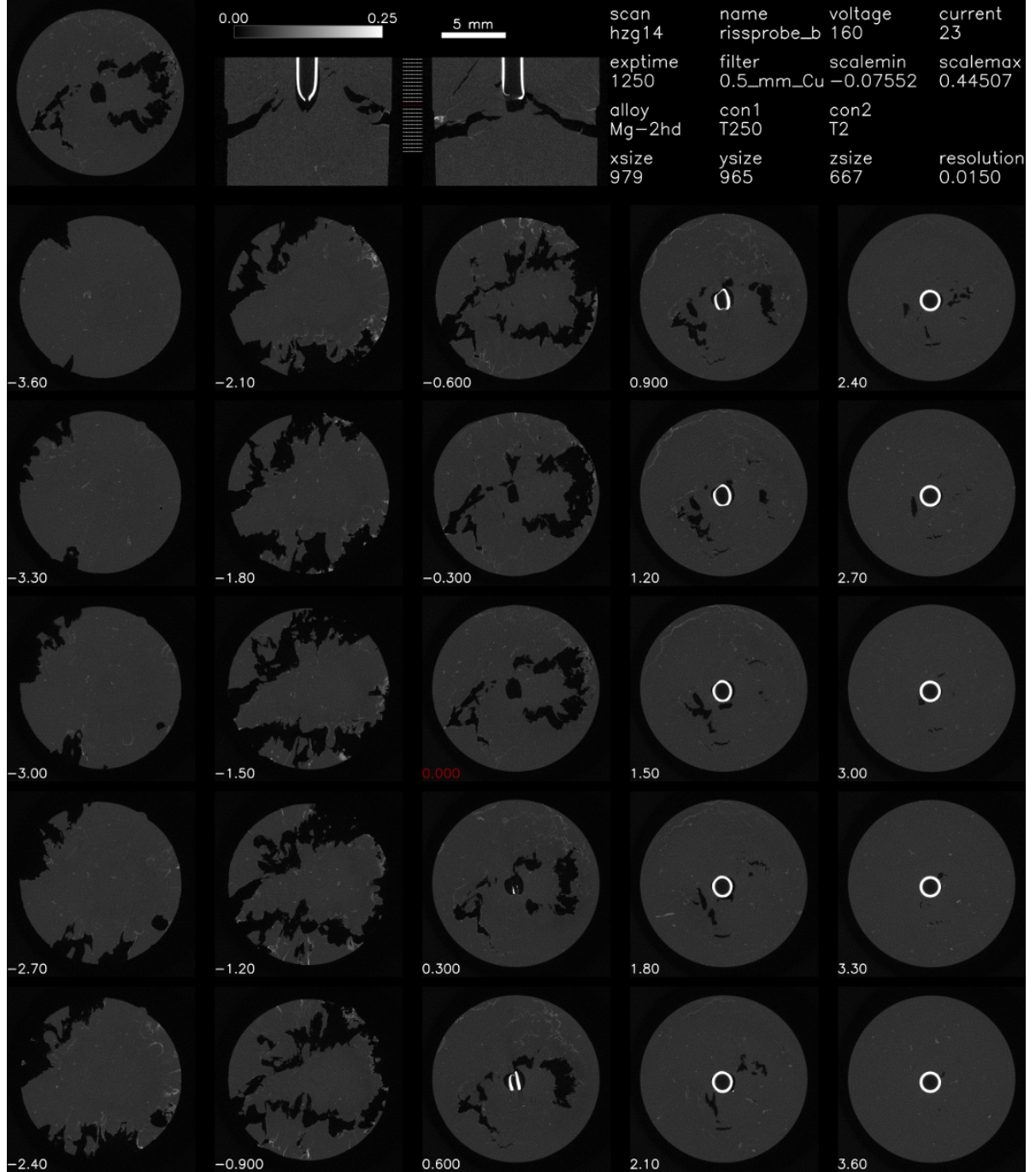


Figure 10: The subsequent slides through the magnesium alloy element.

Examples of slides generated from volume renderings of various samples (Fig. 11) indicate that investigated samples differ in the number and volume of cracks but also in absorption properties.

The obtained results show that the characteristics of occurring cracks in different samples are really diverse and depend on the magnesium alloy composition and casting conditions. In some samples hardly any cracks appear (see samples a and 1 in Fig. 11), for others only small cracks are observed (see sample 10 in Fig. 11), however for some samples many large cracks occur (see samples b, 3 and 8 in Fig. 11).

The difference in absorption properties is probably due to different alloys composition and different concentration of the added heavy elements. Moreover, the images obtained for some samples (see samples a, 1, 10 in Fig. 11) show the occurrence of the inclusions of highly absorbing material. These inclusions appear mostly at the sample surface.

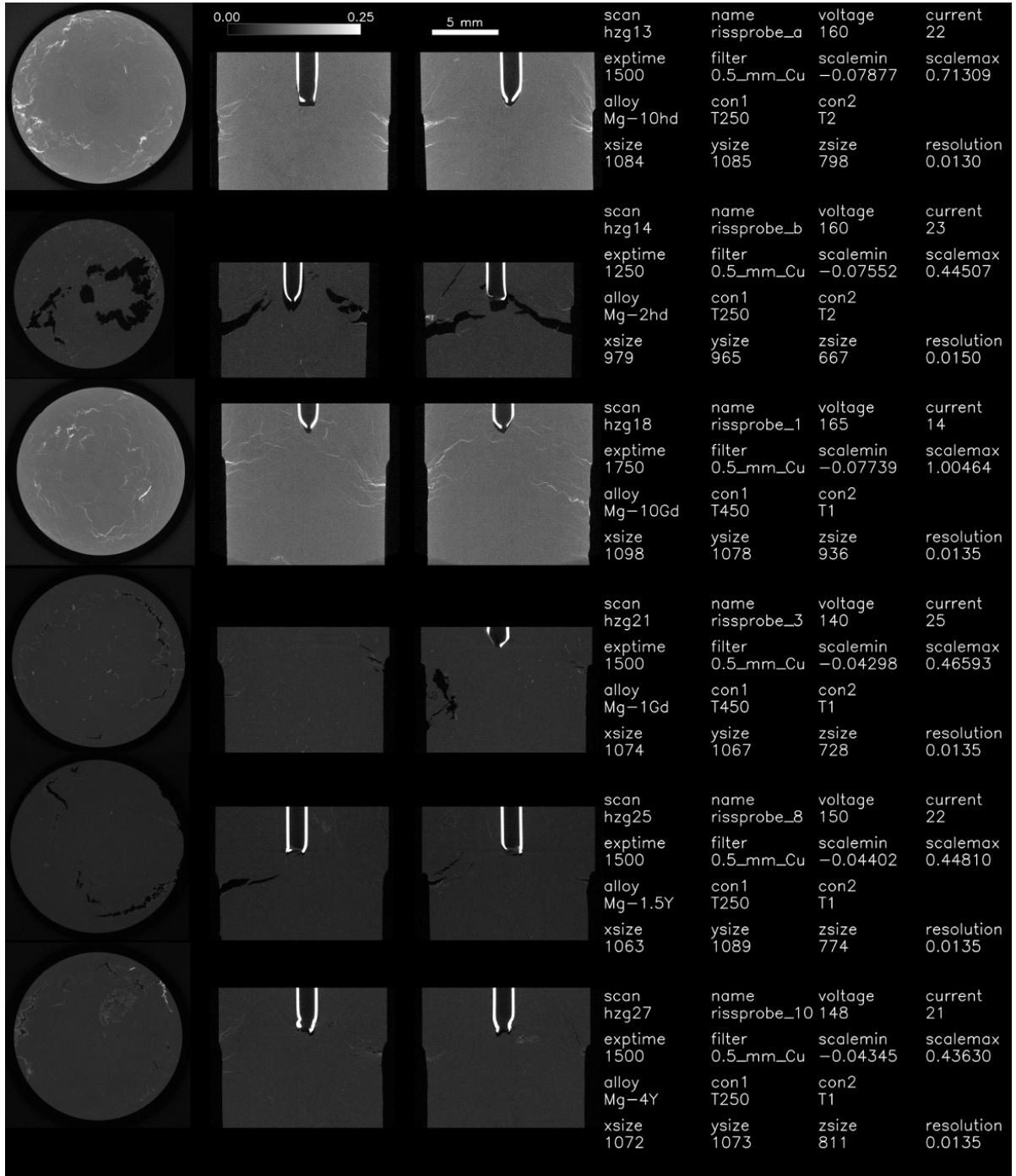


Figure 11: The summary of three different perpendicular slides and scan parameters for various magnesium alloy samples.

6 Conclusions

In conclusion microtomography is a very precise and widely applied technique, which allows the investigation of the 3D microstructure of materials. 3D microtomographic reconstruction allows evaluation of quality, composition and morphology of materials.

Microtomography study of friction stir welding samples has shown the difference in the distribution and number of titanium particles depending on welding speed. This difference may indicate various material flow mechanism for different welding speeds.

The results obtained for magnesium alloy samples show diverse cracks characteristics and diverse absorption properties for different samples. The samples properties depend on the detail alloys composition and casting conditions. The microtomography study of magnesium alloy samples gives opportunity to determine cracks appearing during magnesium alloy process, its number, volume and distribution.

Our results will be discussed by the research groups that are conducting research on friction stir welding and magnesium alloys process.

7 Acknowledgements

We would like to thank Felix Beckmann for scientific supervision, as well as Malte Ogurreck and Fabian Wilde for their invaluable assistance in our studying of the special software, as well as the whole tomographic research group (especially Thomas Dose) for providing us with a unique opportunity to making the experiments, and of course Olaf Behnke and Andrea Schrader who organized the summer student programme 2011.

References

- [1] www.m-osaka.com/fsw
- [2] www.wikipedia.org/wiki/Friction-stir-welding
- [3] Beckmann F., Herzen J., Haibel A., Muller B., Schreyer A., "High density resolution in synchrotron-radiation-based attenuation-contrast microtomography", *Proc. of SPIE* **7078** (2008)
- [4] Beckmann F., "X-ray tomography", *DESY Summer Student Lecture* (2011)
- [5] www.ge-mcs.com/en/radiography-x-ray/ct-computed-tomography.html
- [6] Kak A., Slaney M., "Principles of Computerized Tomographic Imaging", *Society of Industrial and Applied Mathematics*, 2001